Polarimetric Modeling of Atmosphereless Solar System Bodies

Karri Muinonen[1,2], Antti Penttilä[1], and Gorden Videen[3]

[1]Department of Physics, University of Helsinki, Finland
[2]Finnish Geodetic Institute, Masala, Finland
[3]Space Science Institute, Boulder, Colorado, U.S.A.

POLARIMETRY OF PLANETARY SYSTEMS, Villa Il Gioiello, Arcetri
September 23−26, 2013

Contents

- Introduction
- Radiative transfer (RT) and coherent backscattering (CB)
- Phenomenological fundamental scatterer
- Inversion algorithms
- Application to asteroid polarimetry
- Conclusions

Introduction

- Physical characterization of asteroids
- Direct problem of light scattering by regolith particles with varying size, shape (structure), and refractive index (optical properties)
- Inverse problem of retrieving physical properties of particles based on observations
- Plane of scattering, scattering angle, solar phase angle

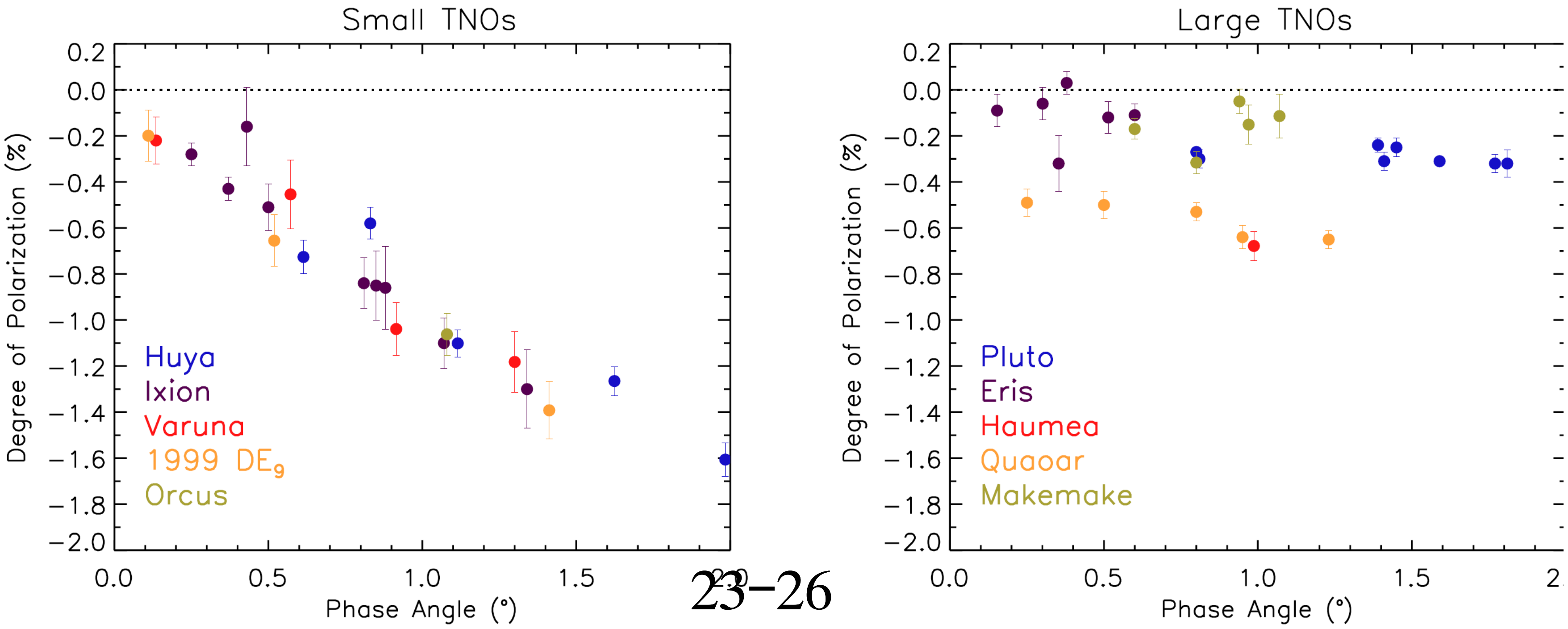

Figure 1: Polarimetry for small TNOs (left—Boehnhardt et al. 2004; Bagnulo et al. 2008; Belskaya et al. 2012) and large TNOs (right—Kelsey and Fix 1973; Breger and Cochran 1982; Avramcuk et al. 1992; Bagnulo et al. 2006, 2008; Belskaya et al. 2008, 2012). Observations mainly obtained at the ESO Very Large Telescope.

Photometric phase curves

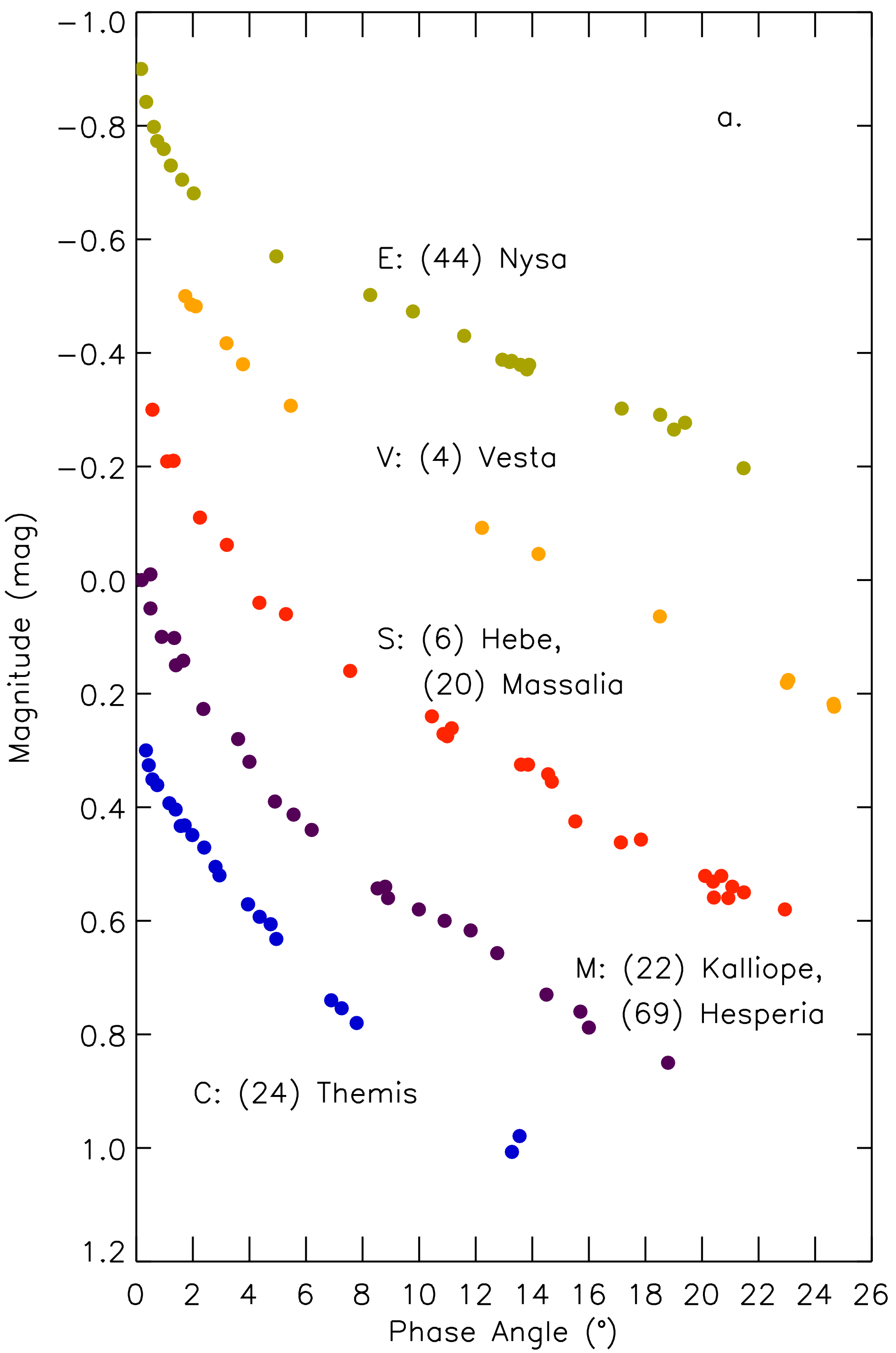

Muinonen et al., in Asteroids III, 123, 2002 (obs. ref. therein)

Polarimetric phase curves

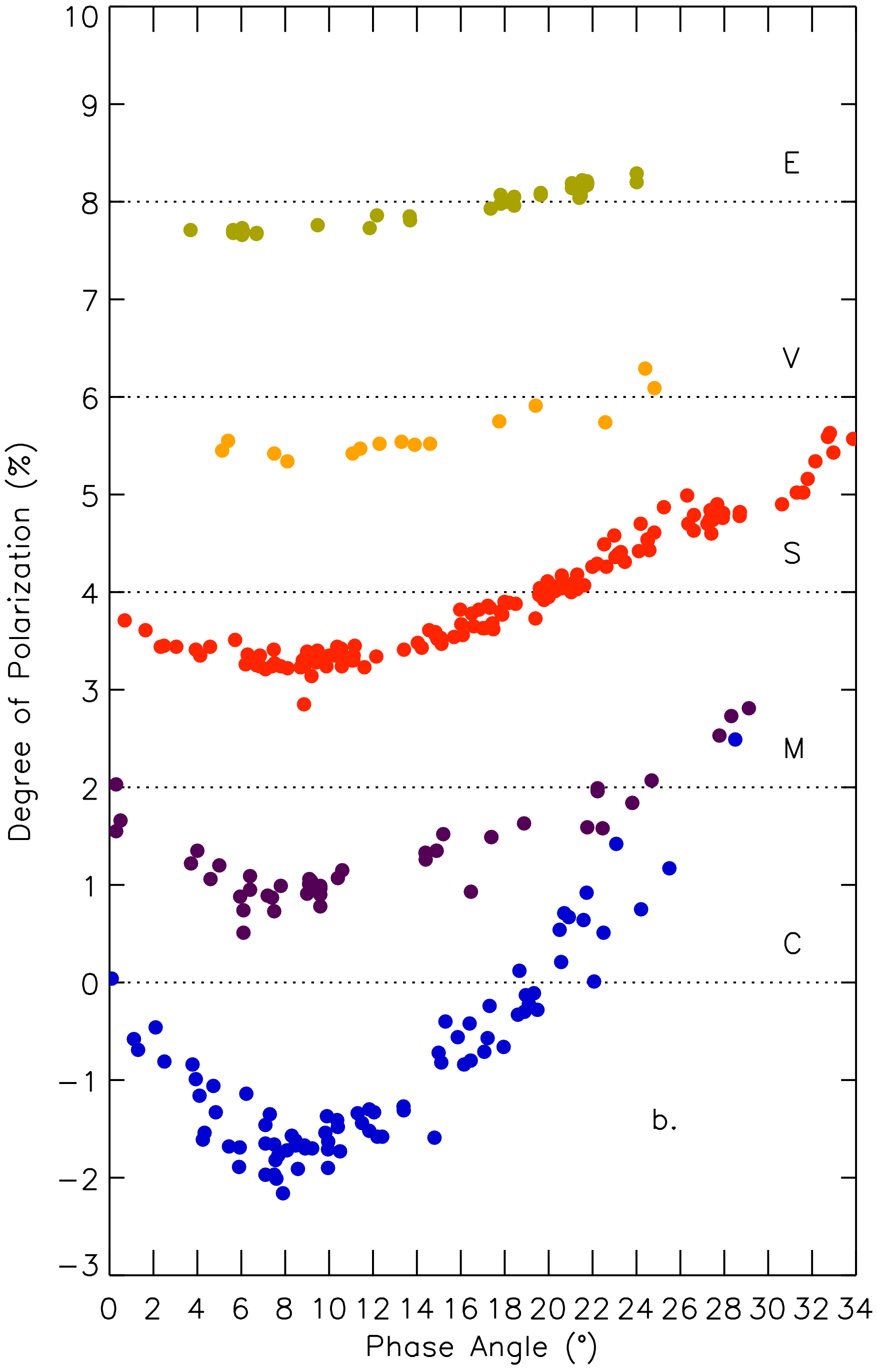

Muinonen et al., in Asteroids III, 123, 2002 (obs. ref. therein)

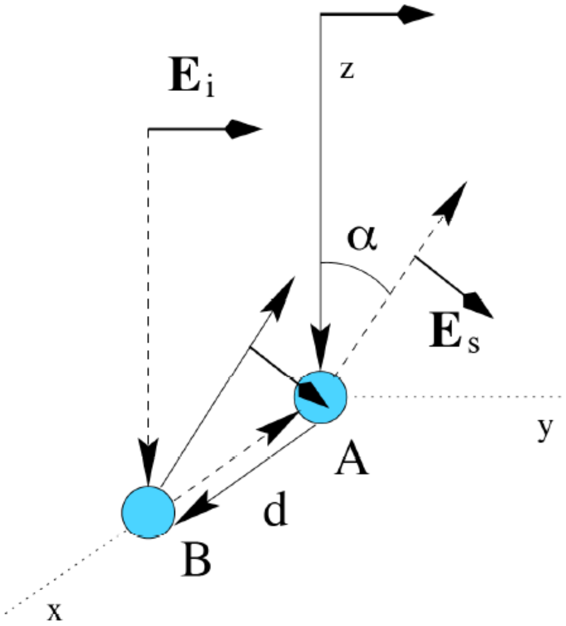
E_i
z
α
E_s
A
B
d
y
x

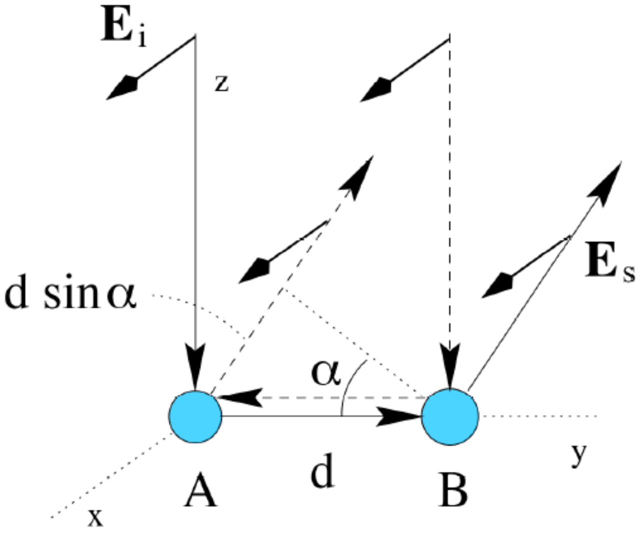
E_i
z
d sin α
α
E_s
A
d
B
y
x

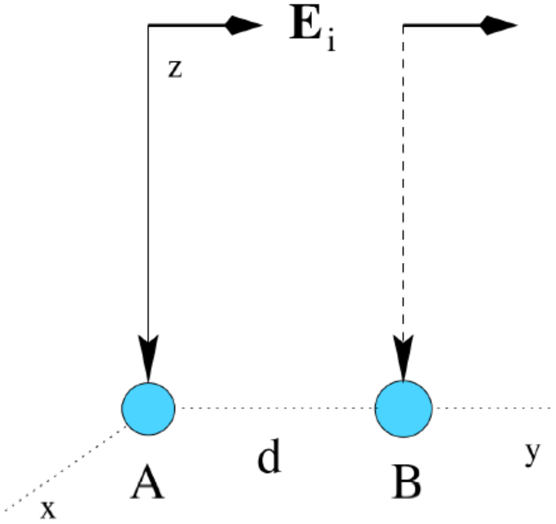
E_i
z
A
d
B
y
x

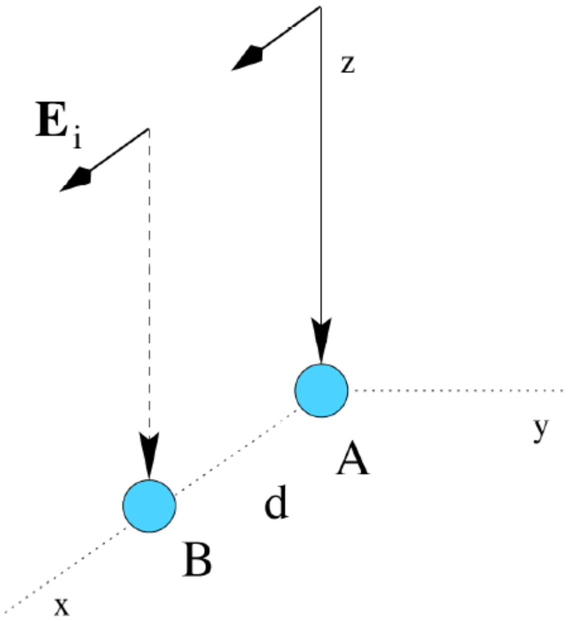
E_i
z
A
y
d
B
x

Radiative transfer & Coherent backscattering

- Polarization and intensity surges due to interference in multiple scattering for a spherical medium
- Monte Carlo computation
- Full angular profiles for the complete scattering matrix

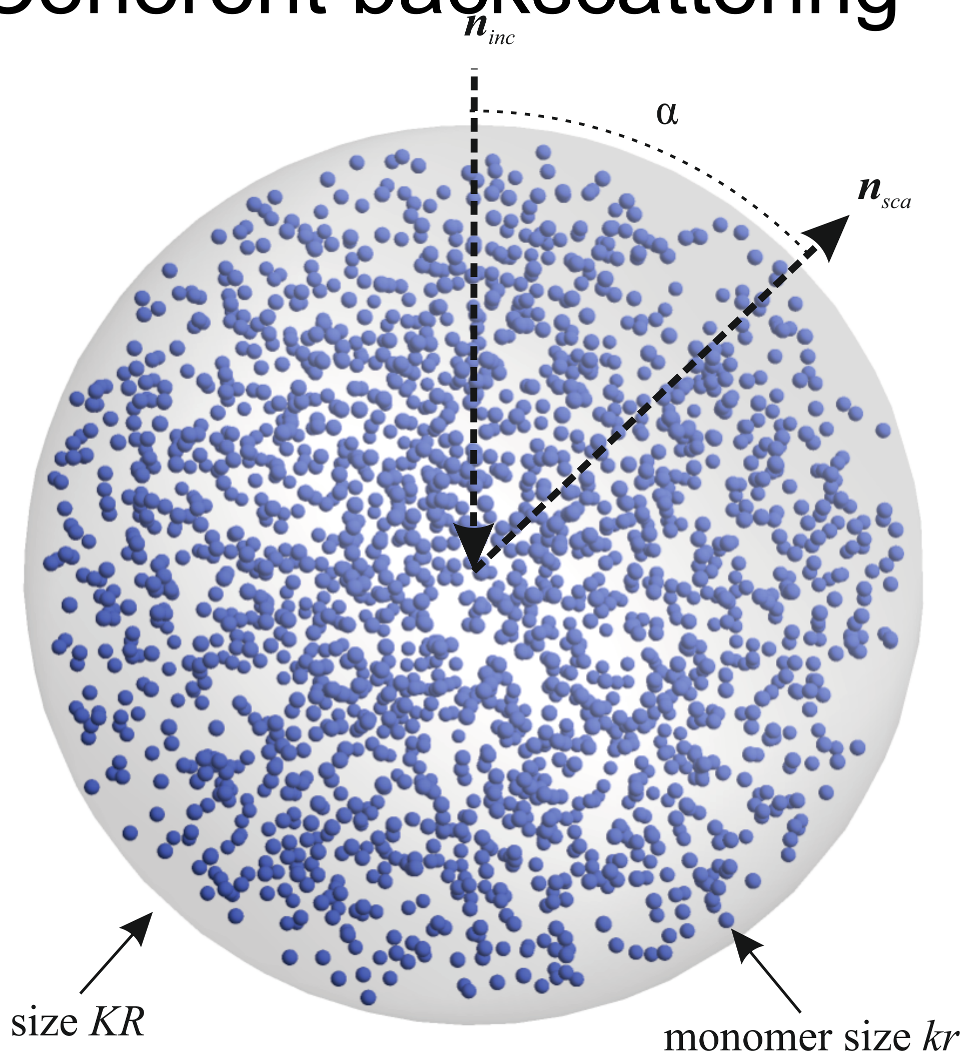

e.g., Muinonen et al., ApJ, 2012

Stokes vectors

$$\boldsymbol{I}_{\mathrm{i}} = (I_{\mathrm{i}}, Q_{\mathrm{i}}, U_{\mathrm{i}}, V_{\mathrm{i}})^T$$

$$\boldsymbol{I}_{\mathrm{s}} = (I_{\mathrm{s}}, Q_{\mathrm{s}}, U_{\mathrm{s}}, V_{\mathrm{s}})^T$$

scattering matrix $\boldsymbol{S}$

$$\boldsymbol{I}_{\mathrm{s}} = \frac{1}{k^2 R^2} \boldsymbol{S} \cdot \boldsymbol{I}_{\mathrm{i}}$$

(Here *R* is the distance between observer and scatterer.)

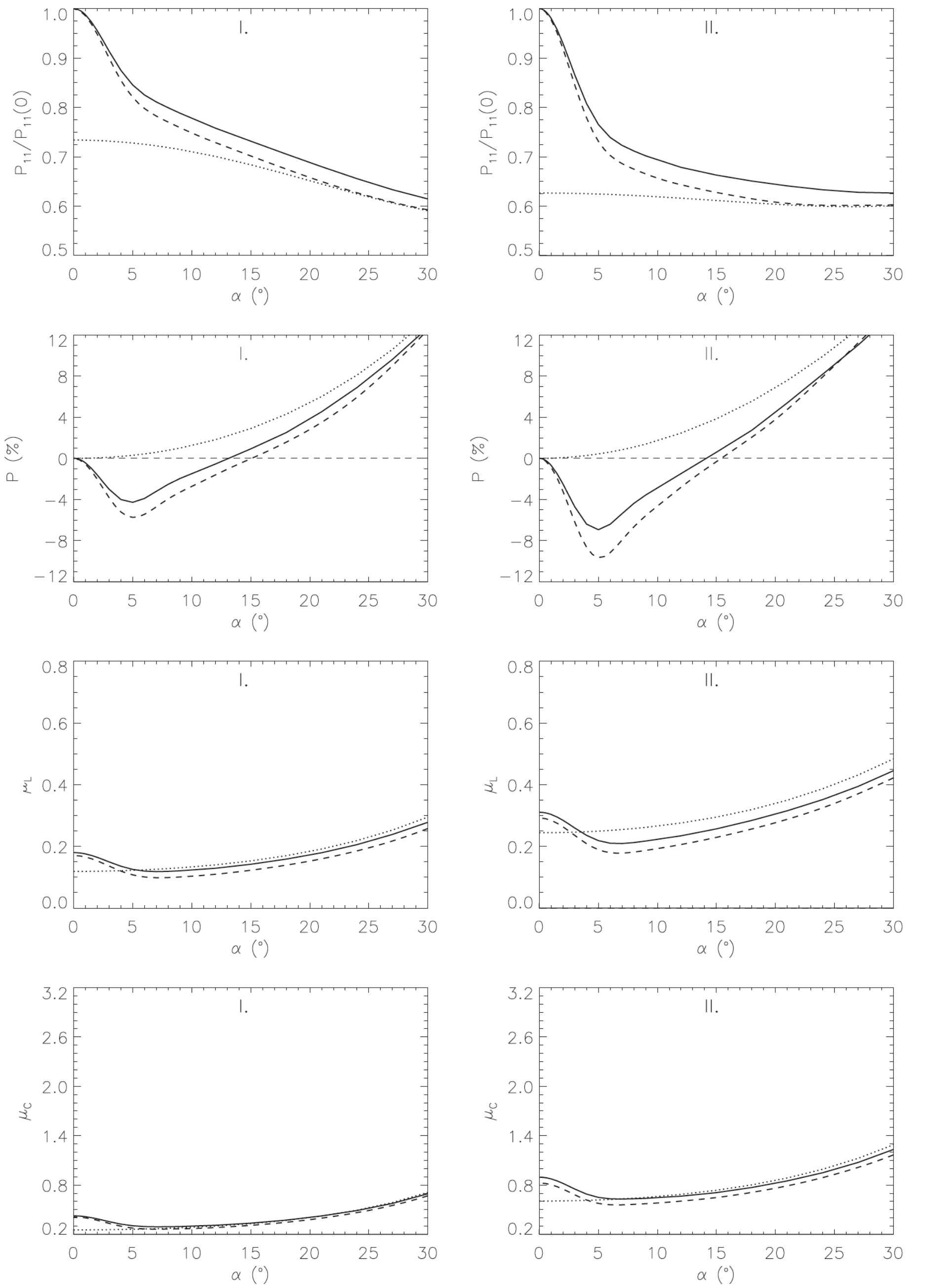

Figure 2. Scattering by a spherical volume of particulate medium with a size parameter $kR = 40$ and packing density of $v = 3.125\%$ (I) and 6.250% (II), populated with spherical particles with a size parameter $kr = 2$ and a refractive index $m = 1.31$. The solid, dotted, and dashed curves depict the RT–CB, RT-only, and STMM results, respectively. See the text.

$$\mu_L = \frac{P_{11} - P_{22}}{P_{11} + 2P_{21} + P_{22}}.$$

$$\mu_C = \frac{P_{11} + P_{44}}{P_{11} - P_{44}}.$$

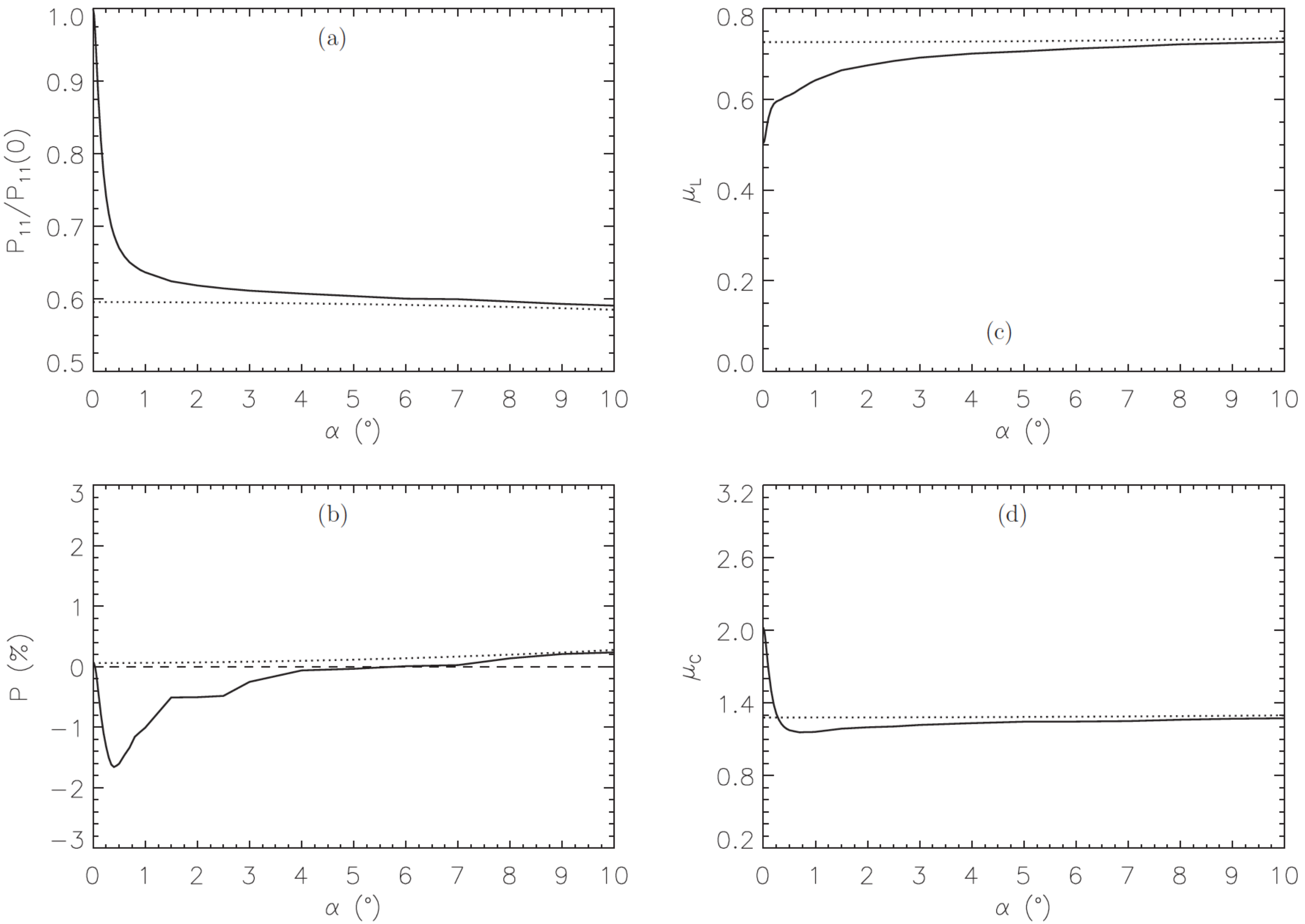

Figure 6. RT–CB (solid lines) and RT-only computations (dotted lines) for a macroscopic medium with $kR = 10^7$ composed of a power-law size distribution (index $\nu = 3$) of spherical monomers with sizes within $kr \in [2.0, 3.0]$. The refractive index of the monomers is $m = 1.31 + \mathrm{i}10^{-3}$ and the volume density is $v = 3.125\%$. (a) $P_{11}/P_{11}(0)$, (b) $P = -P_{21}/P_{11}$, (c) $\mu_\mathrm{L} = (P_{11} - P_{22})/(P_{11} + 2P_{21} + P_{22})$, and (d) $\mu_\mathrm{C} = (P_{11} + P_{44})/(P_{11} - P_{44})$.

RT-CB scattering model

- Radiative transfer, coherent backscattering
- Particulate medium of spherical volume elements and fBm roughness
- Phenomenological fundamental scatterers
- References:
  - Muinonen & Videen, JQSRT 2012
  - Muinonen et al., A & A 531, A150, 2011
  - Parviainen & Muinonen, JQSRT 2007 & 2009
  - Muinonen, Waves in Random Media 14, 365, 2004

Planetary regoliths

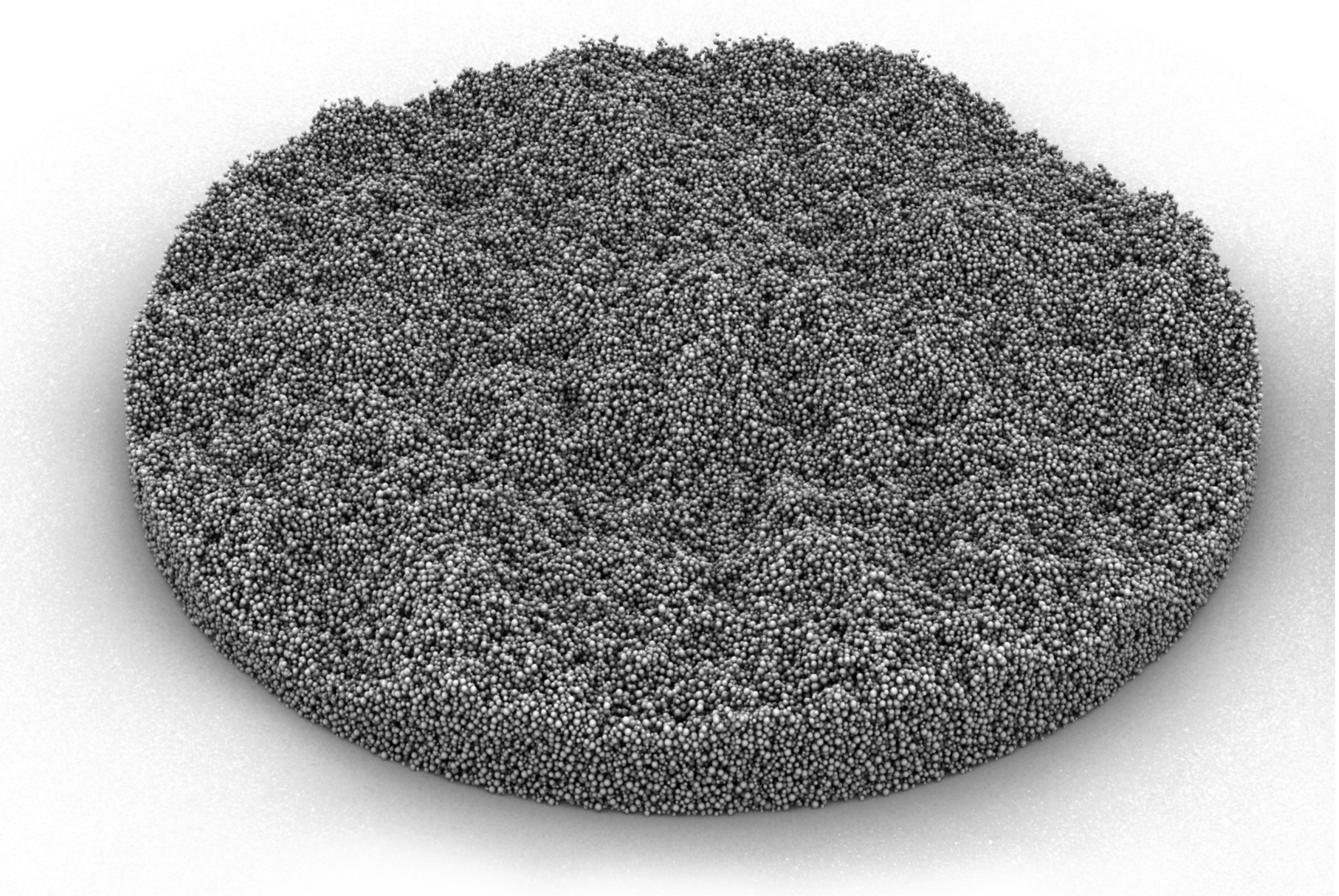

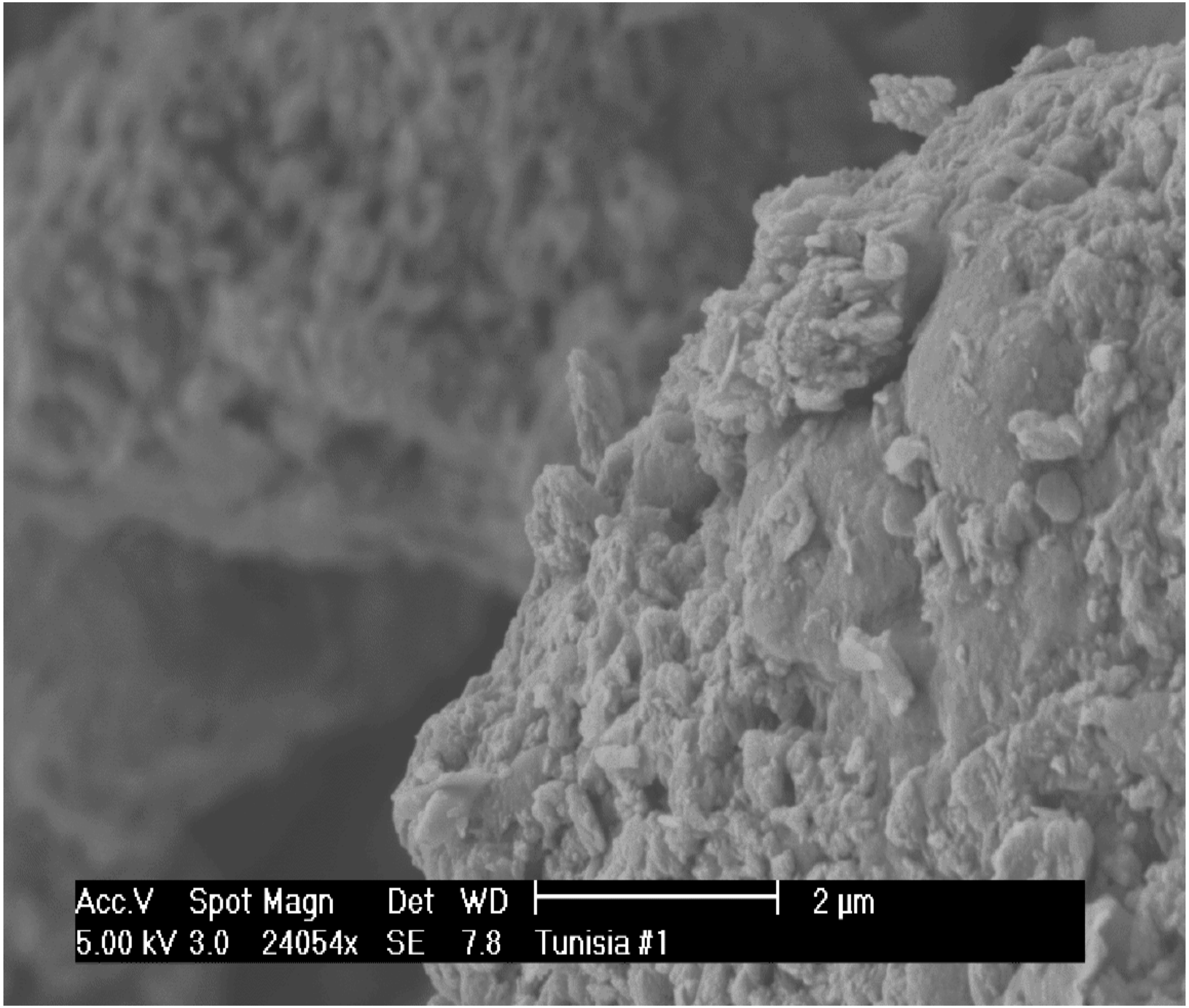

Examples of regolith particles. (Courtesy: Timo Nousiainen)

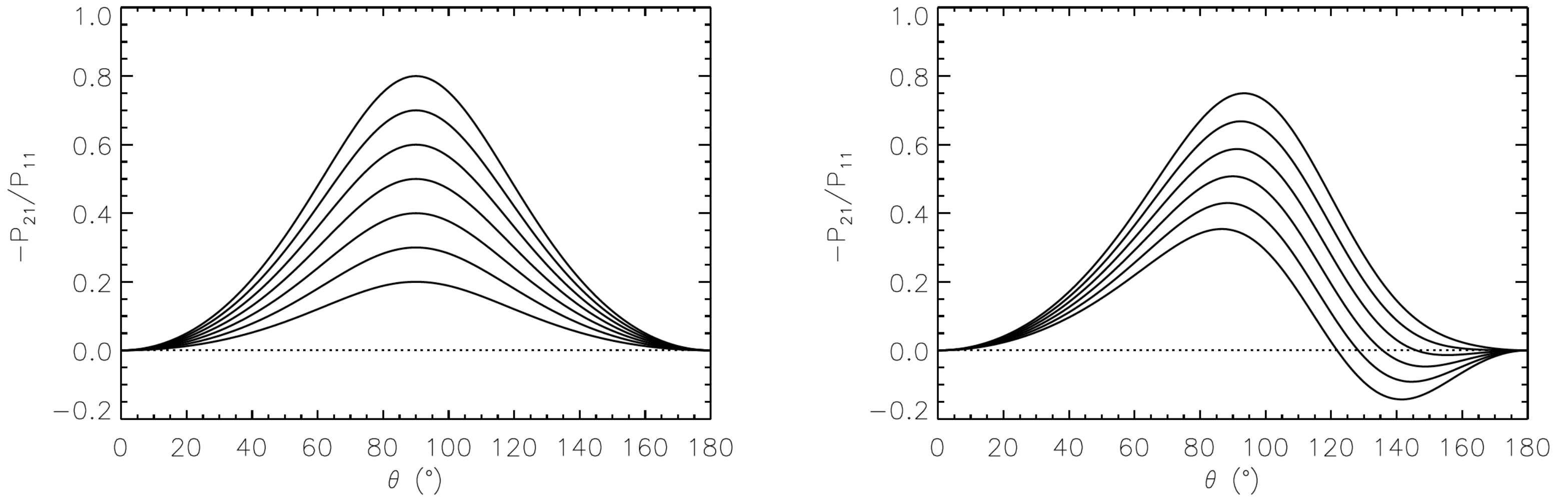

Figure 2: For the single-scatterer polarizations $-P_{12}/P_{11}$ on the left, we have $e_+ = e_- = 0$ and $P_{\rm max} = 0.2, 0.3, \ldots, 0.8$. For $-P_{12}/P_{11}$ on the right, the eccentricities are $e_+ = -0.1$ and $e_- = -0.6$ and the weights are $w_+ = 1 - w_- = 0.60$, $0.65, 0.70, \ldots, 0.85$. With increasing w_+ , the polarization $-P_{12}/P_{11}$ increases.

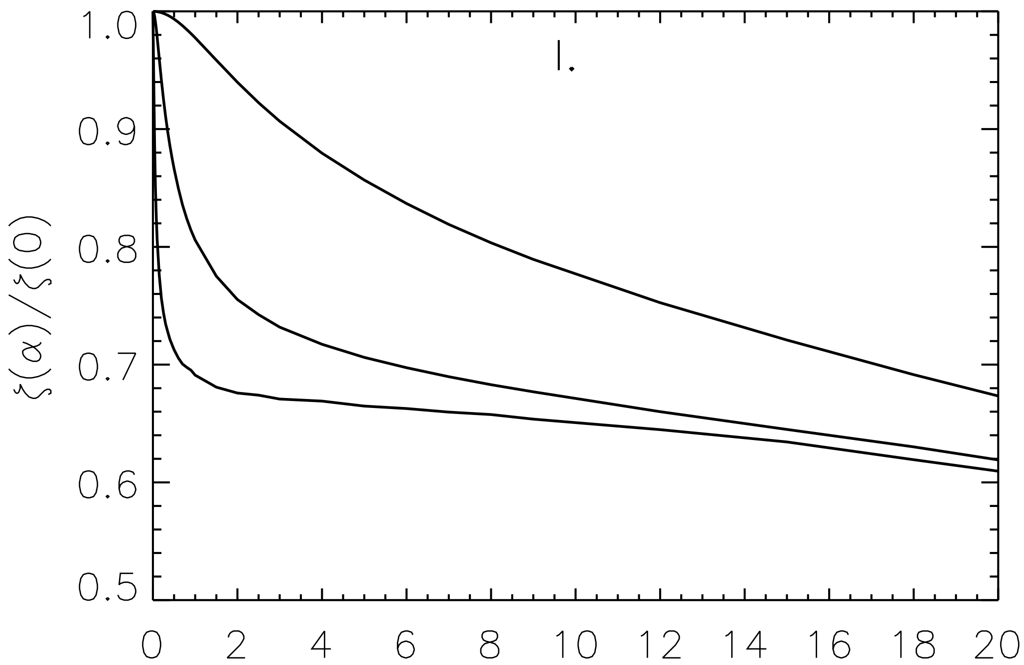

$\tilde{\omega} = 0.6$

$X = 10^7$

$g = 0.6$

$g_1 = 0.8$

$g_2 = -0.1$

$\tilde{\omega} = 0.9$

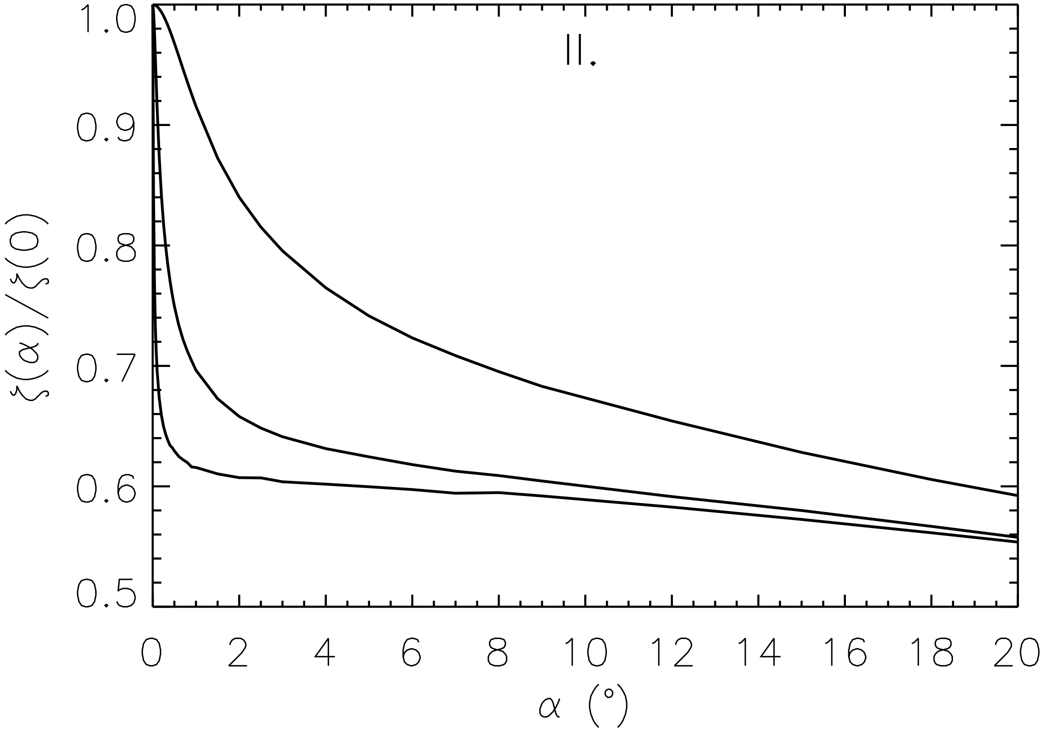

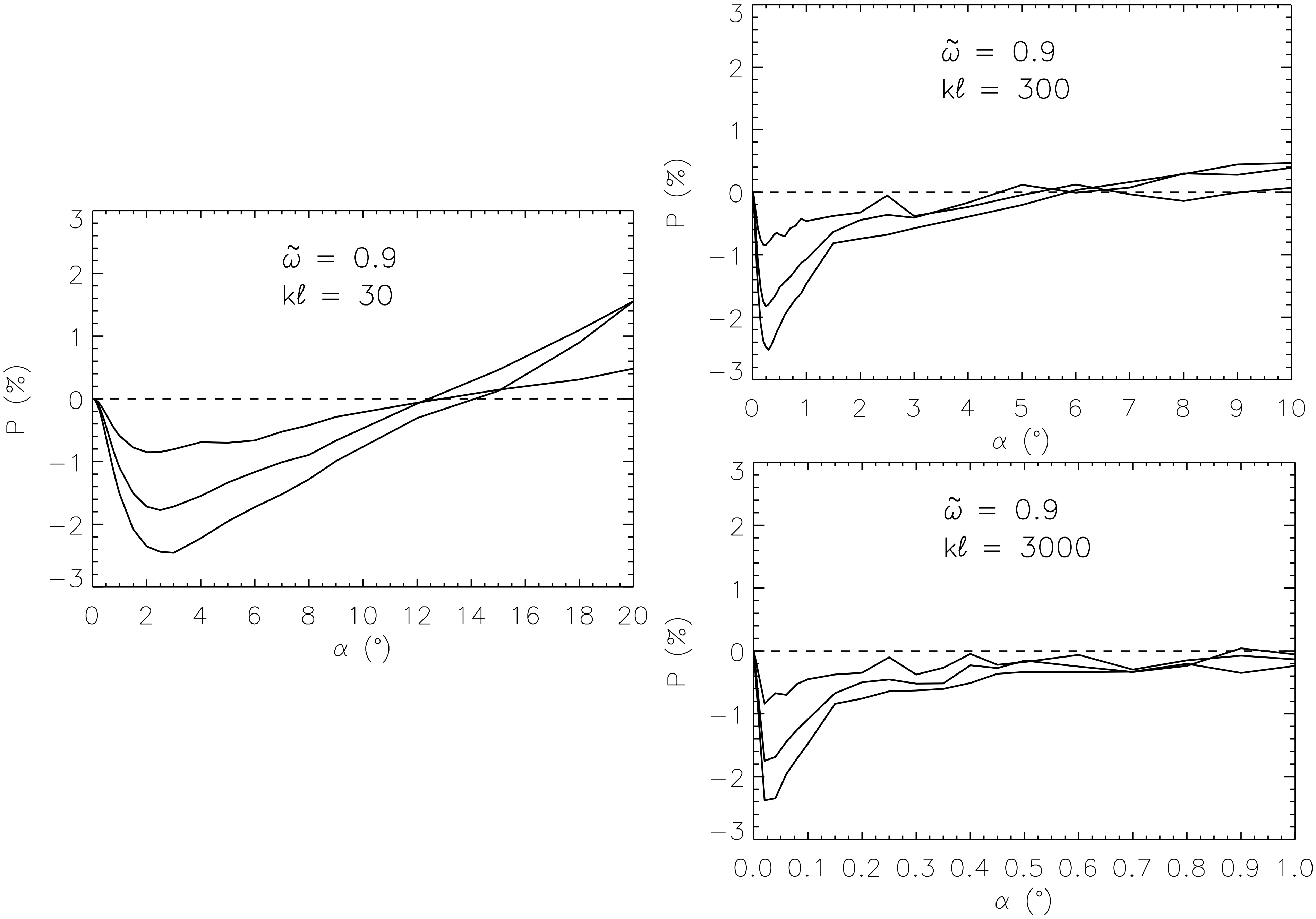
$\tilde{\omega}$ = 0.9
kℓ = 30
P (%)
3
2
1
0
−1
−2
−3
0 2 4 6 8 10 12 14 16 18 20
α (°)
$\tilde{\omega}$ = 0.9
kℓ = 300
P (%)
3
2
1
0
−1
−2
−3
0 1 2 3 4 5 6 7 8 9 10
α (°)
$\tilde{\omega}$ = 0.9
kℓ = 3000
P (%)
3
2
1
0
−1
−2
−3
0.0 0.1 0.2 0.3 0.4 0.5 0.6 0.7 0.8 0.9 1.0
α (°)

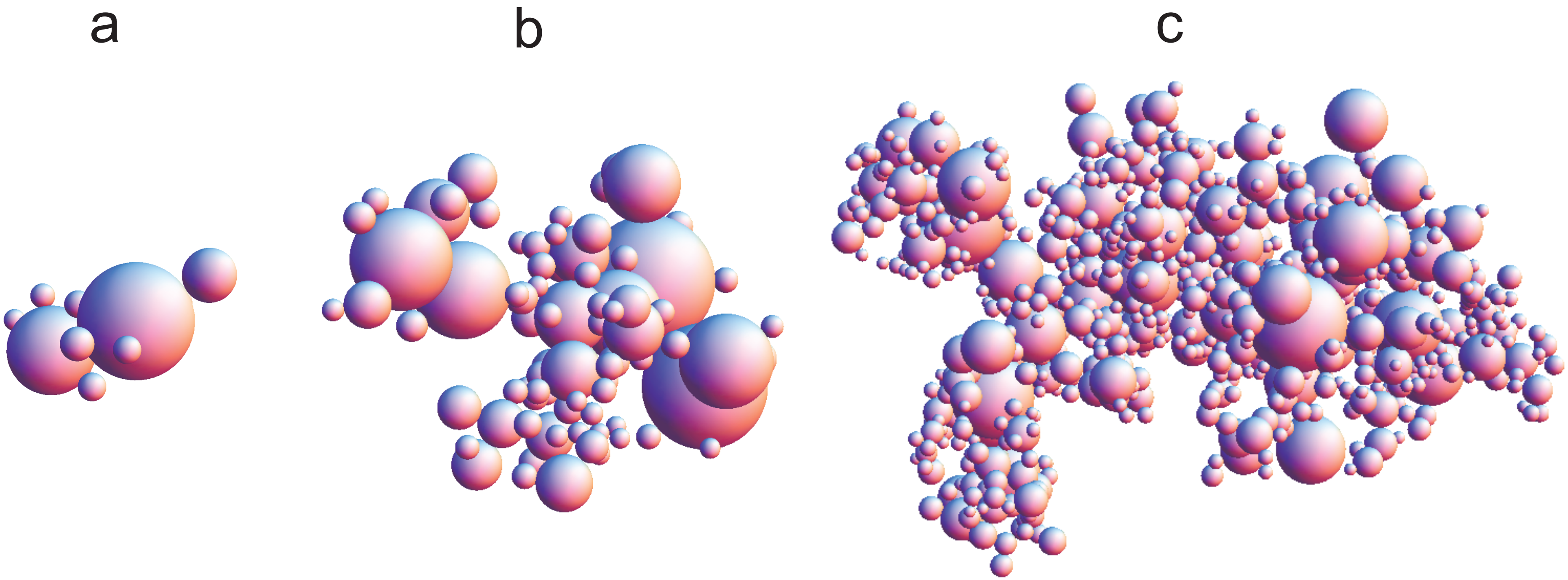

Muinonen et al., RT-CB for close-packed spherical volumes of scatterers, poster on Thursday, this meeting

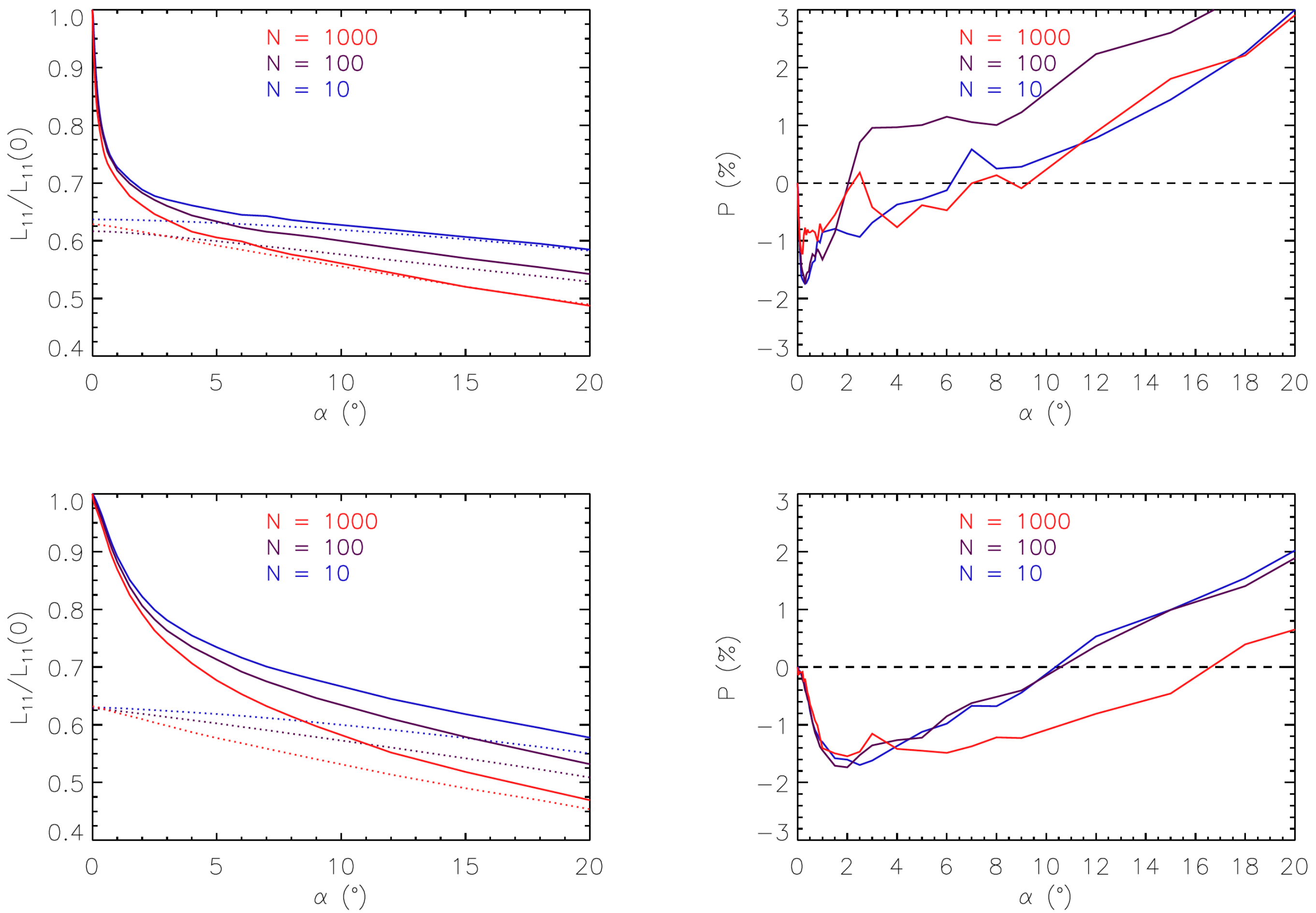

Figure 3: Phase functions (left; dotted lines for RT-only) and degrees of linear polarization (right) for $\tilde{\omega} = 0.9$ in the case of $k\ell = 500$ (top) and $k\ell = 50$ (bottom) for a ballistic aggregate of spherical volumes of scatterers.

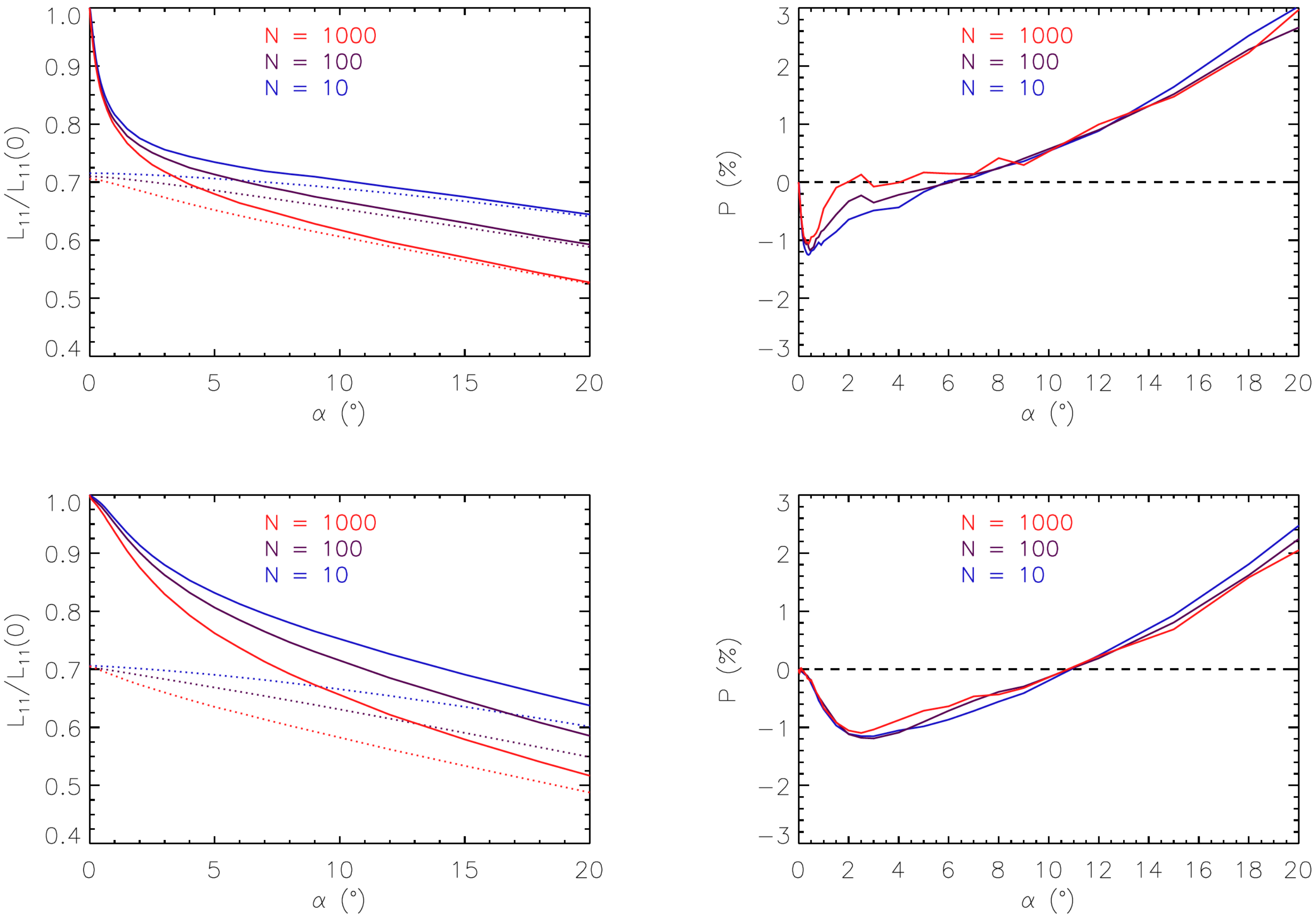

Figure 4: As in Fig. 3 for $\tilde{\omega} = 0.6$.

RT-CB-DDA Inverse Method

- Step 1: Fit the observations using the phenomenological RT-CB model
- Step 2: Fit the phenomenological scatterer using the DDA model (Zubko et al., ADP = agglomerated debris particle)
- Step 3: Optimize the phenomenological against the DDA model
- Convergence
  - NO: Go to Step 1
  - YES: Done

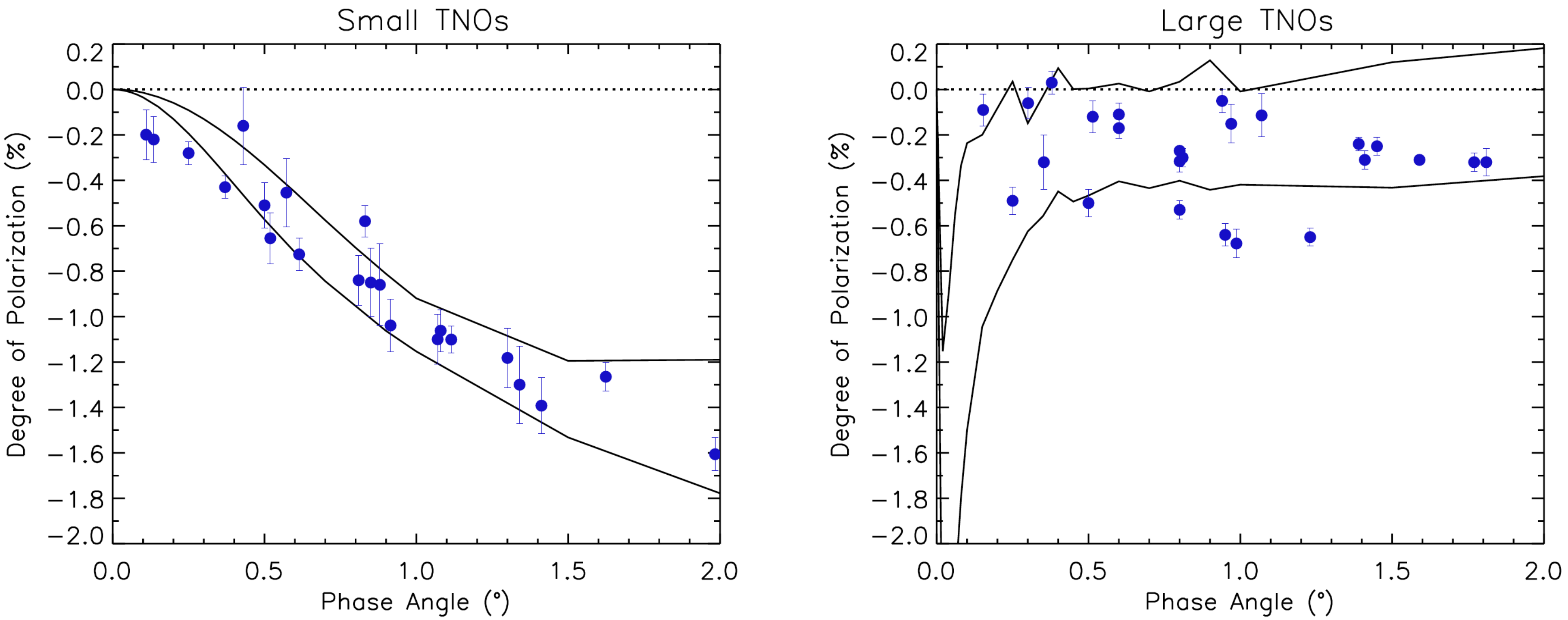

The geometrical albedos p corresponding to the best fits for the small and large TNOs are $p \approx 0.2$ and $p \approx 0.4$. Based on the first analysis, we have $\tilde{\omega} \approx 0.6$, $k\ell \approx 60$ for the small TNOs and $\tilde{\omega} \approx 0.9$, $k\ell \approx 4000$ for the large TNOs. The difference can be due to the presence and absence of volatiles in the surfaces of large and small TNOs, respectively (cf. Bagnulo et al. 2008).

Muinonen et al., DPS 2012

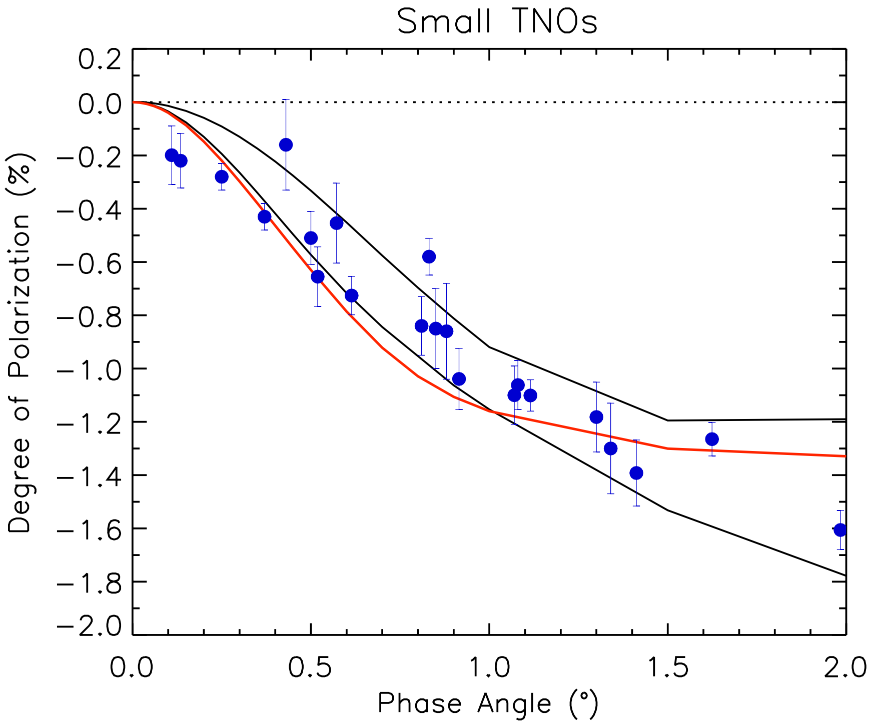
Small TNOs

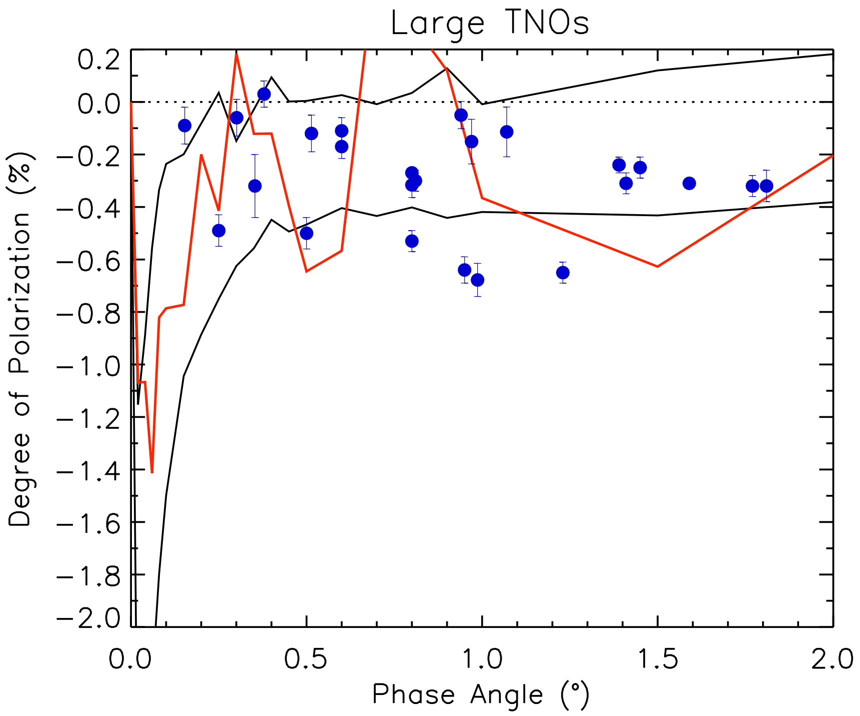
Large TNOs

ADP-model for small TNOs

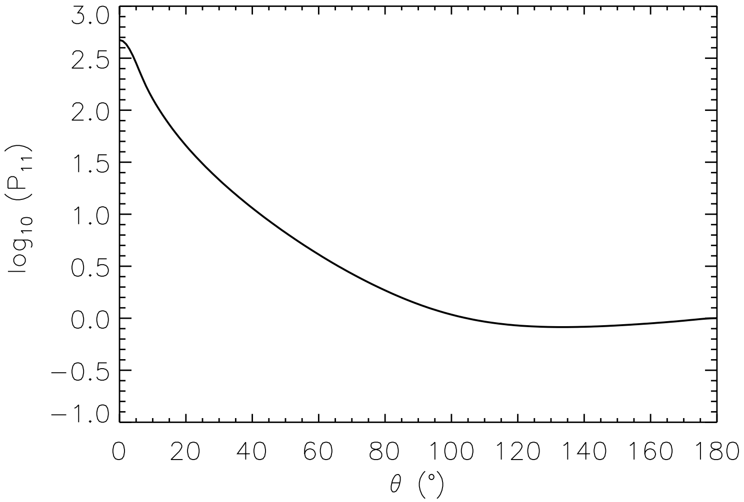

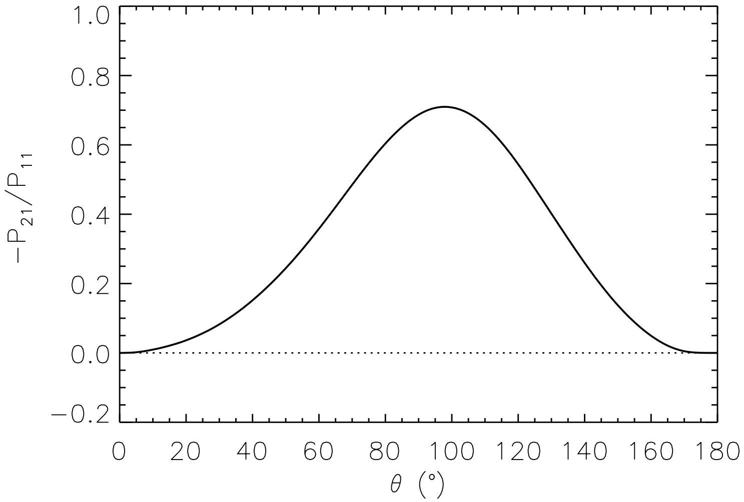

E. Zubko: Dirty ice, $m = 1.40 + i\,0.05$, power law index 3.9

ADP-model for large TNOs

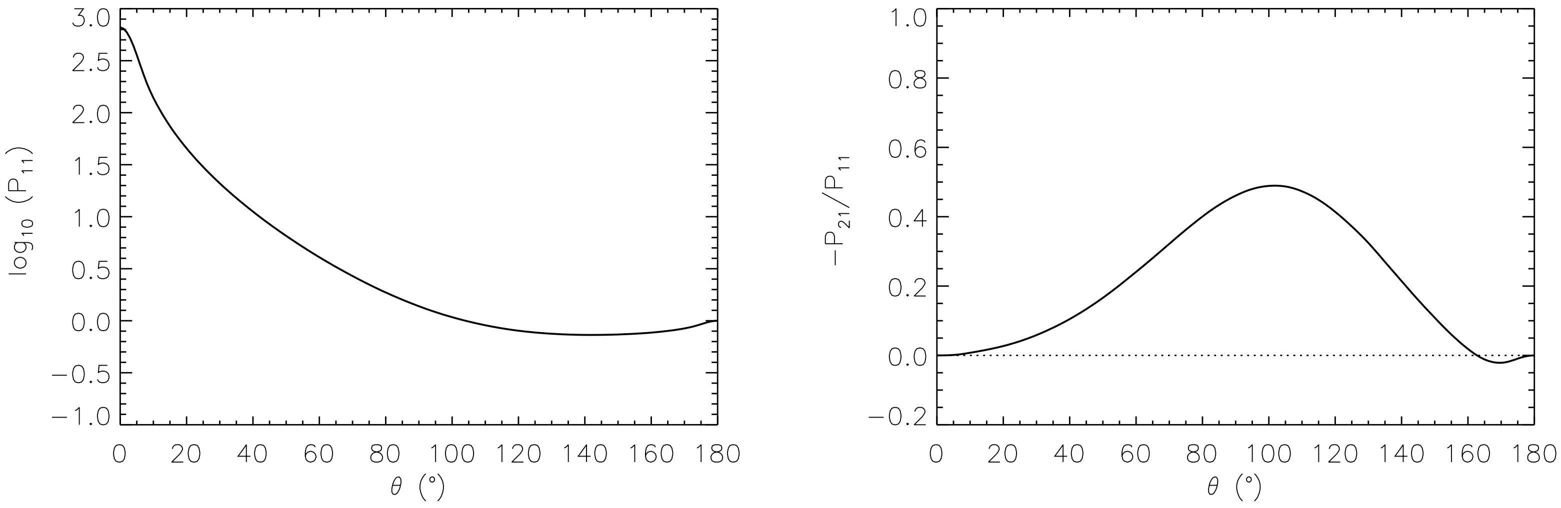

E. Zubko: Dirty ice, m = 1.40 + i 0.02, power law index 3.4

Conclusions

- RT-CB numerically verified for a finite volume of spherical scatterers using MSTM
- Phenomenological RT-CB scattering model capable of fitting the observations
- Iterative modeling of the phenomenological single scatterer allows for the retrieval of optical properties of single scatterers
- Future prospects: regolith geometry to be accounted for, including shadowing effects

Acknowledgments

- Research funded, in part, by
  - ERC Advanced Grant No 320773 entitled "Scattering and Absorption of Electromagnetic Waves in Particulate Media" (SAEMPL)
  - Academy of Finland (contract 257966)
  - NASA Outer Planets Research Program (contract NNX10AP93G)
  - NASA Lunar Advanced Science and Exploration Research Program (contract NNX11AB25G).